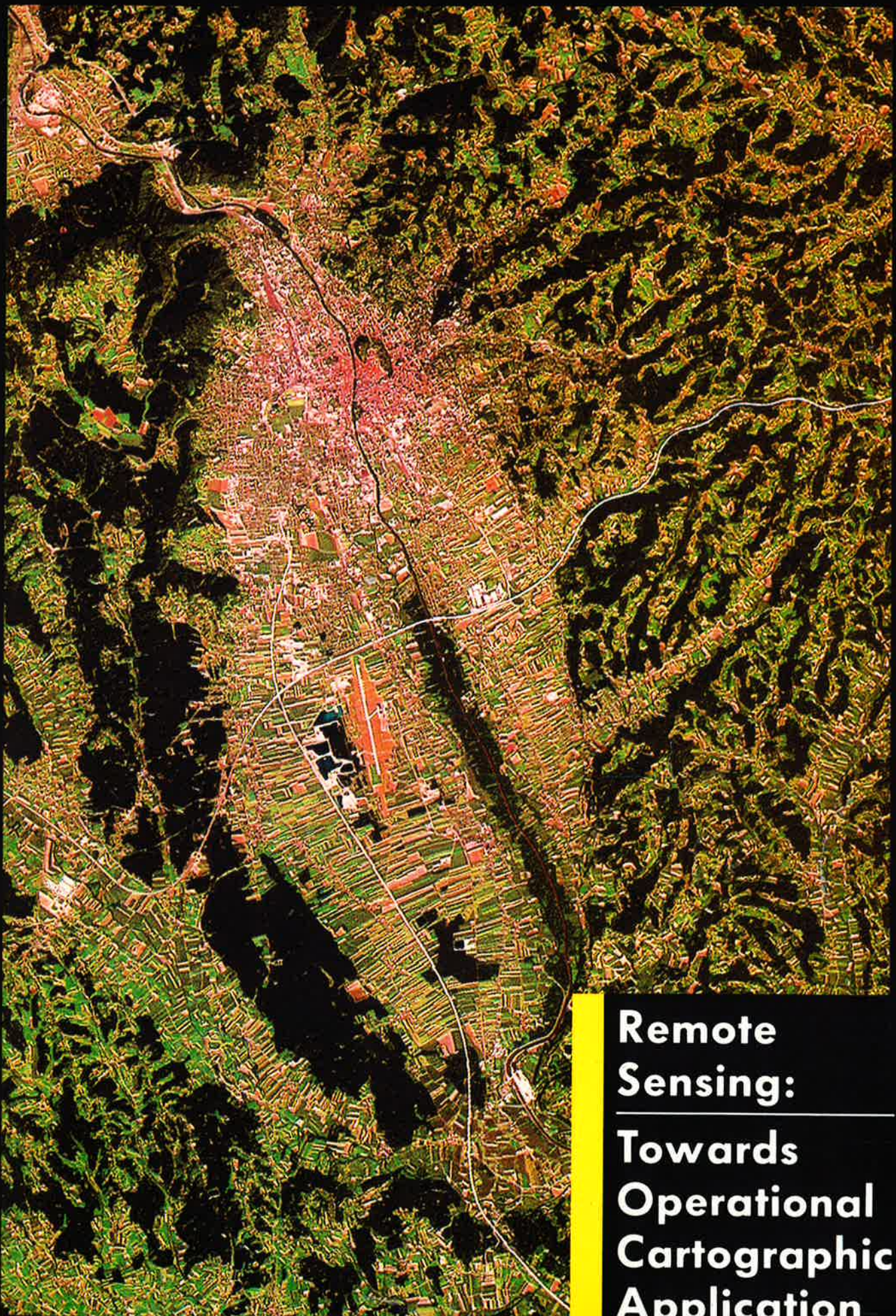


**From left:**

Manfred Buchroithner, organizer of the 1987-Nordberg-Symposium | Franz Leberl, Speaker  
Viktor Kaufmann, Winner of the Nordberg Award | Members of the Nordberg Family





**Remote  
Sensing:**  

---

**Towards  
Operational  
Cartographic  
Application**



M.F. BUCHROITHNER  
and R. KOSTKA (Ed.s)

**Remote Sensing:**  

---

**Towards Operational  
Cartographic  
Application**

Proceedings of the  
**WILLI NORDBERG SYMPOSIUM 1987**  
held in Graz, Austria, 7-9 September 1987

Organized by  
Graz University of Technology  
Forschungsgesellschaft Joanneum, Graz  
Center of Earth Resource Management Applications,  
Springfield, VA



Forschungsgesellschaft Joanneum  
**Institute for Image Processing and Computer Graphics**  
Graz

# SOME MAPPING APPLICATIONS FOR DIGITAL SAR IMAGERY

F. W. Leberl

Vezcel Corporation  
Boulder, Colorado, USA

## ABSTRACT

The interest in mapping from SAR images is currently increasing. This is due to a number of planned Earth remote sensing satellite systems such as ESA's ERS-1, Japan's ERS-1, Canada's Radarsat, NASA's SIR-C and EOS. This paper reviews recent SAR mapping technology as applied to 1:50,000 image mapping from airborne digital SAR, SIR-B research and sea-ice mapping.

Keywords: Radargrammetry, Shuttle Imaging Radar, Sea-ice Kinematics, Radar Image Mapping.

## 1. INTRODUCTION

Synthetic Aperture Radar (SAR) data collection is currently nearly entirely digital. Therefore a range of digital image processing capabilities is now available for data analysis and transformation that was not applicable to film-imagery.

The technological advances are accompanied by an increased interest in SAR remote sensing; this interest is essentially based on the well-known all-weather, day-and-night operation of radar sensors. The European, Japanese, Canadian and US Space Agencies all are preparing for various SAR satellite missions (Table 1). This is accompanied by high performance aircraft SAR at 2m to 6m slant range and azimuth resolution, supported not only by inertial navigation but by Global Positioning System measurements (GPS) as well.

We report in this paper on three SAR mapping activities to illustrate recent advances in the applications of SAR. We will first present STARMAP, a technique to create 1:50,000 image maps from airborne SAR images. This is followed by a discussion of automated sea-ice mapping with SAR. Finally we report on the radargrammetric work with SIR-B imagery in Argentina and Australia.

## 2. TOPOGRAPHIC IMAGE MAPPING AT SCALE 1:50,000 WITH AIRBORNE SAR (STARMAP)

### 2.1 General Observations

Classical standards of cartographic mapping from imagery put demands on image scale for planimetric and height accuracy as well as image contents for interpretation. This has been discussed in detail in an earlier paper (Leberl, 1982). Planimetric

Table 1: Satellite SAR projects currently in preparation

Mission	Agency	Status	Expected Launch
E-ERS-1	European Space Agency	Approved	1990
J-ERS-1	Japanese Space Agency	Approved	1992
Radarsat	Canadian	Approved	1992
SIR-C	U.S. NASA	Approved	1991
EOS	U.S. NASA	Pending	1994
Magellan	U.S. NASA	Approved	1989

accuracy usually is the least of all constraints since it deals with presentation at an output map scale at a graphical accuracy of  $\pm 0.2\text{mm}$ ; in smaller map scales such as 1:50,000 an allowance is made for map generalization and accuracies of  $\pm 0.5\text{mm}$  are acceptable.

A map 1:50,000 would thus be expected to have root mean square errors of  $\pm 25\text{m}$ .

Height is a scale-independent factor: height is symbolized by a numerical code to contour lines and spot heights. One may usually find 10m contour intervals at scales 1:50,000 and 20 m if the terrain is accentuated. Flatlands may even be depicted by 5m contour lines. This puts a demand on the height accuracy from stereo-imagery to produce height values with errors smaller than 1/3 of the contour interval (or 1/5 by European cartographic standards). For a 20 m contour interval, height accuracy ought to be better than 7m.

The most critical factor for mid to small scale mapping at 1:50,000 is image detail to identify bridges, roads and other man-made features. A rule-of-thumb of photogrammetric literature relates map and image scales as follows

$$m_1 = 250 * m_2^{1/2} \quad (1)$$

where  $m_i$  is the image scale number,  $m_m$  the map scale number.

A map scale 1:50,000 would require an image scale of 1:60,000. This needs to be related to SAR-resolution. One such consideration is to equal a line pair to 2.8 pixels, leading to:

$$m_i = 1000 * 2^{1/2} * 2 * n * a \quad (2)$$

where "n" is the resolution of a presentation image in line pairs per millimeter, "a" is the pixel diameter in meters. At  $n = 20$  lp/mm we get

$$m_i = 56,000 * a. \quad (3)$$

An image scale,  $m_i$ , of 1:100,000 would correspond to a pixel size of about 2 meters, 1:50,000 to 1.2m.

## 2.2 SAR Resolution and Accuracies for Classical Mapping

Clearly, SAR resolutions of 6 meters to 30 meters are insufficient for mapping under existing cartographic needs. At least 2 m resolution would be needed under these standards. The SAR height accuracies reported so far in the literature typically are a multiple of ground resolution. Again, therefore, a 7 m height accuracy cannot be met by SAR.

This limitation has long been faced with Landsat data. This caused a new type of product to come into existence, the "image map". This is an ortho image map with or without superimposed contour lines. One generally argues that an ortho image map should have a  $\pm 0.5$  to  $\pm 1.0$  mm planimetric error (25 to 50 m at scale 1:50,000), and the rectified image has to be presented with 3 to 8 pixels per millimeter. At a 6m resolution this leads to map scales of 1:18,000 to 1:48,000. We see that SAR has the resolution for image maps at scale 1:50,000, at planimetric accuracies of  $\pm 25$  to  $\pm 50$  meters.

In order to obtain a rectified SAR image, the topographic relief has to be known so that its effect can be removed from the SAR image. The  $\pm 0.5$  to  $\pm 1.0$  mm accuracy requires terrain heights to be known to about 25m to 100m. This removes topographic effects with errors less than  $\pm 25$ m: the shallow SAR look angles off-nadir will often reduce the relief effects by a factor of 4. Therefore the height accuracy from stereo SAR may be sufficient for rectification, but insufficient for contouring commensurate with 1:50,000 rules.

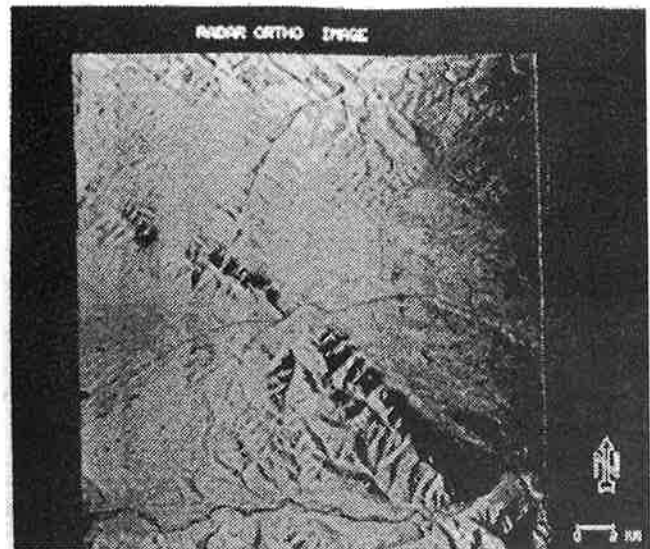
It is entirely obvious then that a SAR mapping product has to be an image map. Such a product is available under the name STARMAP<sup>1)</sup>.

## 2.3 Creation of a 1:50,000 SAR Image Map

An operational procedure has been developed that takes as input a set of overlapping SAR-images and a set of (identified) ground control points. The images are available in both a digital form, and on film.

The film images serve in a stereo-mapping effort to create a digital elevation model (DEM). Figure 1 is a sample image from a demonstration project in Alberta, Canada. Figure 2 is the DEM extracted from the image pairs.

(a)



(b)

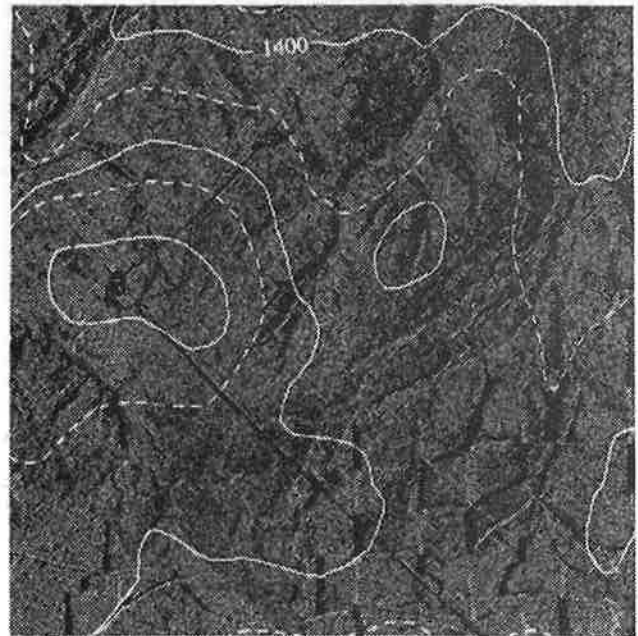


Figure 1: Sample of a SAR image map of one area in the Brazeau range in Alberta, Canada. Flight height was 8.5 km above ground, wavelength 3 cm, resolution is 6m x 6m, look angles off-nadir range from 50° to 70°. Contour interval is 50 m: (a) overview, (b) detail.

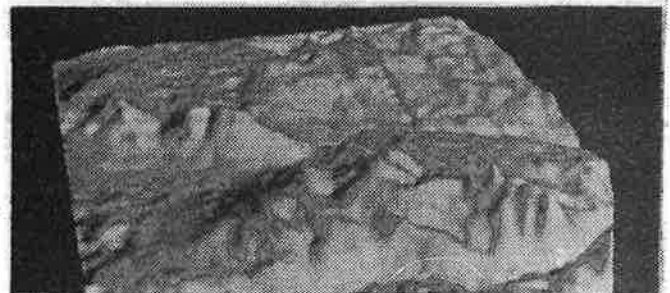


Figure 2: Digital elevation model obtained from the stereo SAR images. Area is 25 x 25 sqkm. The terrain heights range from 1,200 m to 2,000 m. Accuracies are about  $\pm 35$ m (Courtesy E. Kienegger, VEXCEL).

<sup>1)</sup> From INTERA Technologies, Ltd, Calgary, Canada.

Stereo-model set-up and data collection is on a Kern DSR-11 with program SMART, an experimental software system developed at the Graz Research Center. The specifics of the hard- and software were reviewed in a paper by Raggam and Leberl (1984). Height data are collected in grid form and supplemented by terrain break lines. Collection density is at about a 180m grid spacing, thus at 5 times the height accuracy.

The DEM is a data source for differential rectification of the digital images, and for the computation of contour lines. In order to achieve a planimetric accuracy of  $\pm 25\text{m}$  the topographic heights need to be known to within  $\pm 30\text{m}$  at near range (look angle off-nadir of  $50^\circ$  and to within  $\pm 90\text{m}$  at far range (look angles of  $75^\circ$ ).

The rectified SAR image and contour lines are merged with a map frame to result in the SAR image map.

#### 2.4 Accuracy of a SAR Image Map

With a density of one ground control point per 10 sq km the accuracy of the final mapping product was

- $\pm 29\text{ m}$  in X (northing),
- $\pm 33\text{ m}$  in Y (easting),
- $\pm 35\text{ m}$  in Z (height).

These values were obtained by comparing 16 identifiable features on the final image map with those on a conventional 1:50,000 map of the Canadian national map series.

Independently the SAR derived DEM can be compared to a map-derived DEM. The result is shown in Figure 3. Where shadow areas exist one finds larger DEM-errors, simply since no height values have been measured in the shadow areas. When shadow areas are disregarded then the height errors are found to be about  $\pm 29\text{ m}$ .

#### 2.5 Discussion

There are three areas of technological advancement in the use of SAR for mapping. First, it needs to be pointed out that the described product is the result of using a fairly dense grid of ground control points. The need for such control defeats the purpose of an inexpensive SAR survey. Therefore it is necessary to drastically reduce the use of ground control and to employ inertial navigation and global positioning. Secondly it seems awkward to have digital SAR data, yet to require them to be recorded on film to use an analytical photogrammetric instrument. Efforts need to be made to have stereo mensuration available for softcopy data in a digital image processing environment.

Thirdly, one often refers to SAR data as a means to obtain detailed "topographic expression": this is the result of brightness variations from terrain slopes, as they produce different reflections depending on the orientation to the SAR-antenna. The DEM creation has only been based on geometric parallaxes; it seems promising to also exploit the brightness variations as a source of slope and height information.

Progress is expected in all three areas in the near future.

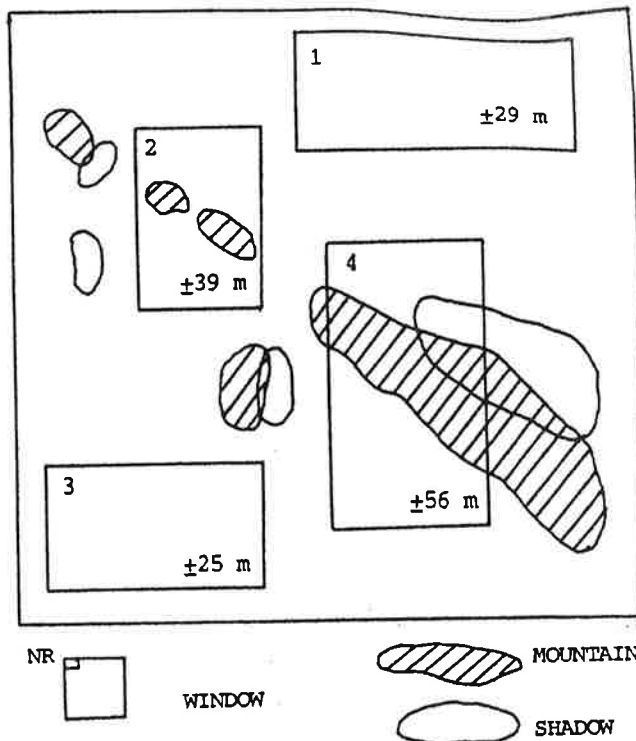


Figure 3: The difference of the SAR- and map-derived DEMs is computed per window by subtracting the two height values in each DEM-location. The windows are marked, with the corresponding r.m.s. DEM differences in meters. Note that shadow areas contribute a large error to the r.m.s. values.

### 3. SEA-ICE KINEMATICS FROM SATELLITE SAR

#### 3.1 The Problem

Sea-ice motion has long intrigued oceanographers, glaciologists, meteorologists and those operating in arctic regions with ships.

Various attempts have been made to observe sea-ice motion by means of remote sensing. However, weather conditions and long arctic nights have only permitted very small data sets to come into existence.

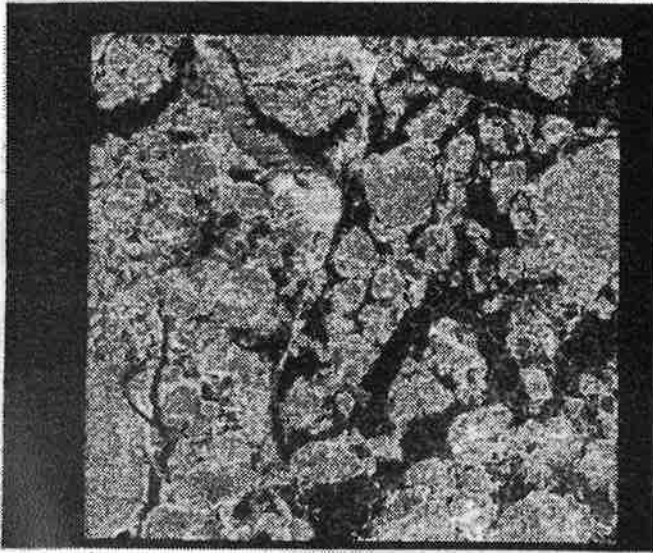
For many years the argument has been made that satellite SAR is the only meaningful observation tool for year-round sea-ice mapping. However, proper polar platforms have not been available. Instead SAR-data are only obtained from sporadic aircraft missions, and for 3 months SEASAT generated a vast arctic data set. These were analyzed for sea-ice motion (for example Leberl et al., 1979,1982), employing manual techniques.

SEASAT and aircraft data are still the only sources for arctic SAR. Upcoming satellite radar projects cause, however, a renewed look into the use of future SAR images for tracking of the moving sea-ice. The ambition is to automate the task.

#### 3.2 Automated Sea-Ice Mapping

We believe that a fully automated SAR kinematic mapping system can be built with current tools. This is being illustrated with numerous SEASAT L-band image pairs. An example is shown in Figure 4.

(a)



(b)

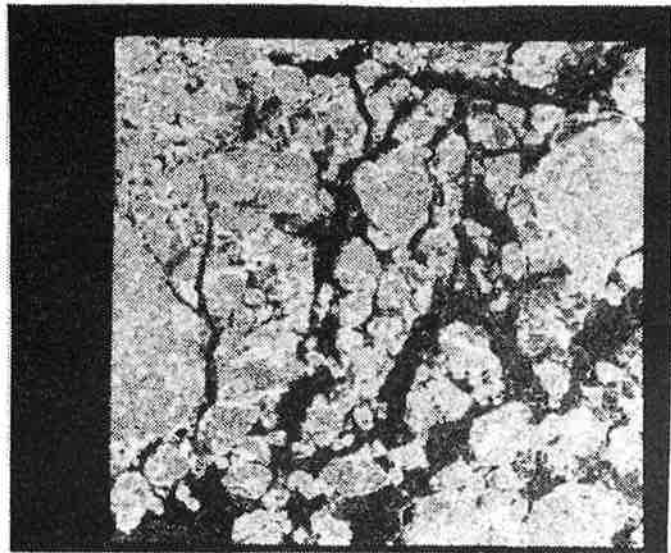


Figure 4: Pair of L-Band SEASAT images of the Beaufort sea, covering 13 x 13 sq km. Images were taken 3 days apart.

There exist numerous concepts for automating the image matching process, most prominently image correlation. However, changes in the ice, its rotation and irregular translation, break-up and melting have led to the proposal to employ "object-oriented" matching rather than "signal-oriented" methods. Vesecki et al. (in print) have demonstrated in the open literature some concepts for successful automation of the ice motion measurement.

Figure 5 is derived from Figure 4 with only the major linear objects such as ice floe boundaries. Rather than matching pixel arrays by 2-d correlation, a method may employ segments of linear objects and look for the matching segment in the other image. Similarity detection can be arranged in a manner that is rotation and translation-invariant. A mere 1-dimensional match of linear objects replaces the 2-d correlation.

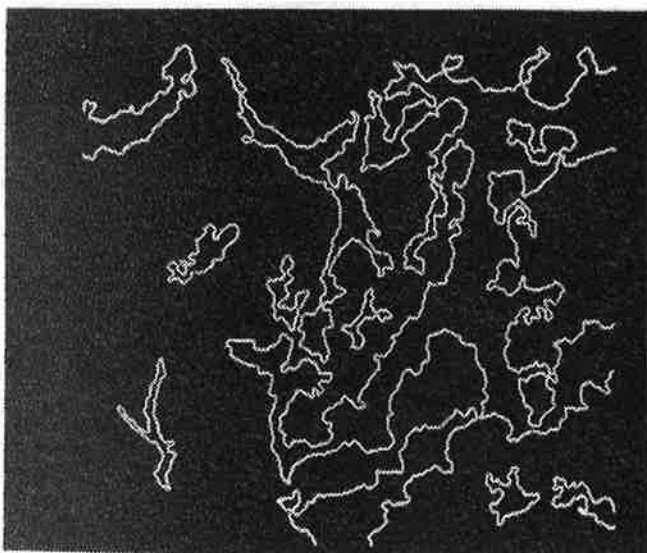


Figure 5: Linear objects extracted from the input image of Fig. 4a. Only the major objects are extracted. The process is fully automated (courtesy R. McConnell, VEXCEL).

Figure 6 presents the result of the automated process: motion vectors indicate the different motions of various image segments.

The entire process is rather elaborate but fast. The extraction of vectors from a 13 x 13 sqkm image patch with 25 m pixels takes less than 2 minutes on a VAX 11/780, without any specific optimization.

An operational implementation is currently under way for a geophysical processing system in Fairbanks, Alaska, for use with future ERS-1 (Europe and Japan) SAR data.

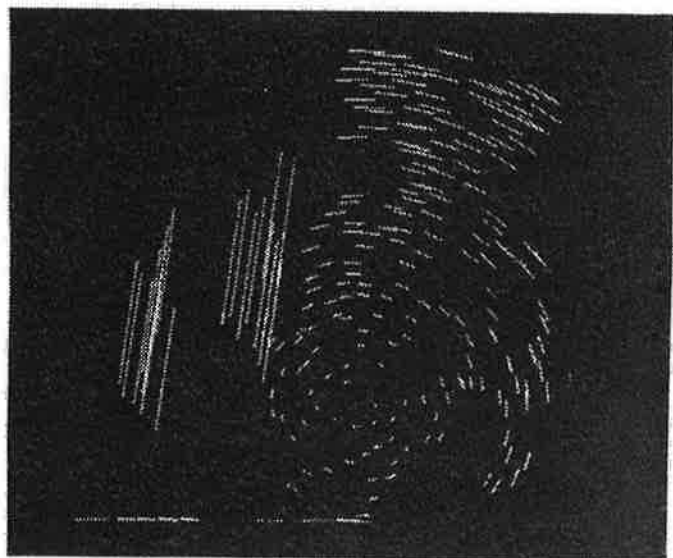


Figure 6: Motion vectors for the SAR image pair of Figure 4a. The vectors are obtained in a fully automated procedure. Note the differences in the motion of various image segments (Courtesy R. McConnell, VEXCEL).



#### 4. RADARGRAMMETRIC ANALYSES OF SIR-B SAR IMAGES

##### 4.1 Data Sets

SIR-B was a SAR data collection effort on board of NASA's Space Shuttle Challenger in October 1984. The resulting data set is unique since it presents repeat coverages of several test sites with differing SAR look-angles off-nadir.

Major test sites with interesting--since mountainous--topography are: Mt. Shasta, California; Argentina; Australia; Illinois; Raisin City, Nevada; and Bangladesh.

The most elaborate data set is of one area in Argentina, where 3 ascending orbit images combine with 2 descending orbit images to a 5-fold coverage.

Figure 7 is a subset of the SIR-B coverage of Jose de San Martin. It does not lend itself to significant geological or vegetation studies, but serves to support the development of SAR mapping methodologies. Together with coverages of other areas it complements the range of stereo-mensuration results obtained from SIR-B.

##### 4.2 Processing Results

All overlapping SIR-B images of non-flat terrain have been analyzed for use in stereo mapping techniques. Table 2 is a summary of the various errors obtained. It appears that a coordinate error of 3 to 4 times the resolution was achievable ( $\pm 50\text{m}$  with  $12.5\text{m}$  pixels, presenting a  $15\text{m}$  range resolution). The results are inconsistent since in some cases a stronger geometry produces poorer results, in other cases the opposite occurs. The inconsistency of the results is hard to explain. While one may be tempted to relate it to the terrain characteristics it is also related to image noise. However, a quantitative analysis of the variations has not been made.

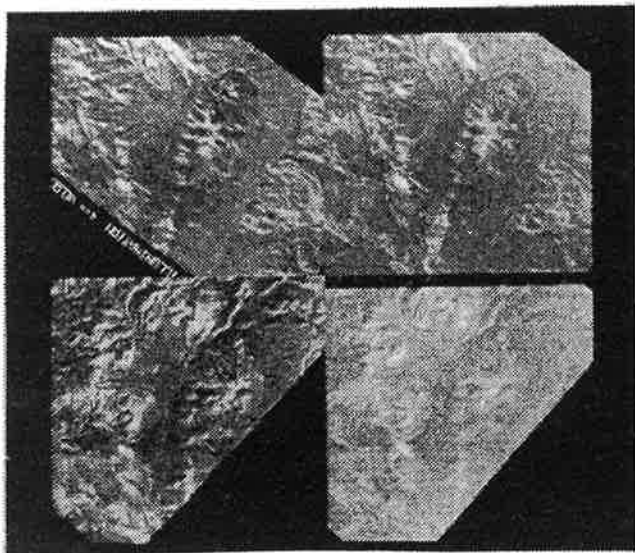
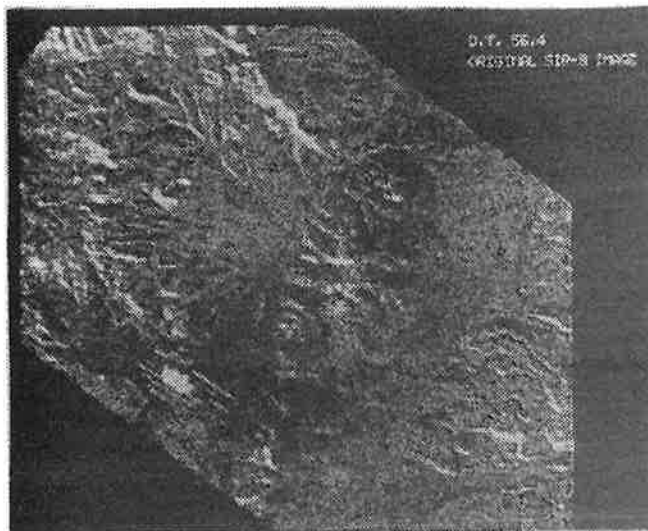


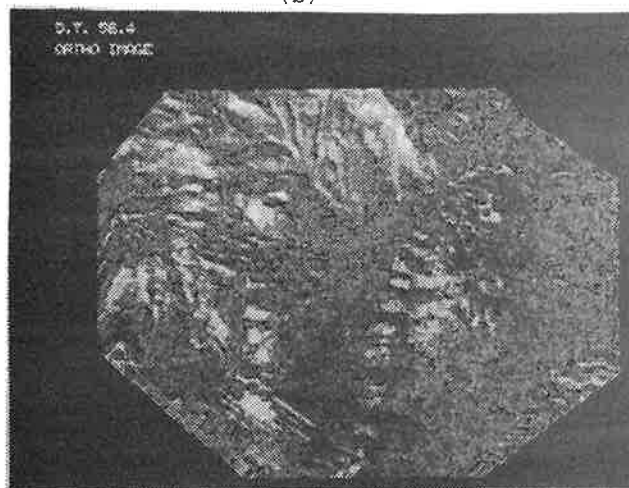
Figure 7: Overlapping coverage from SIR-B of an area in Argentina, Jose de San Martin. Area is  $20 \times 20$  sq kms. SIR-B was L-band, look angles are between  $23^\circ$  and  $50^\circ$  off nadir; (a), (b) are from ascending, (c), (d) from descending orbits.

The DEMs created from SAR can be used for "geo-coding" or rectifying the digital SIR-B data. This may include also radiometric "rectification". Figure 8 is an example, comparing raw and rectified images. If this is repeated with every component image one could obtain a multi-dimensional data set for automated analysis of surface cover, particularly if the images are also radiometrically rectified.

(a)



(b)



(c)

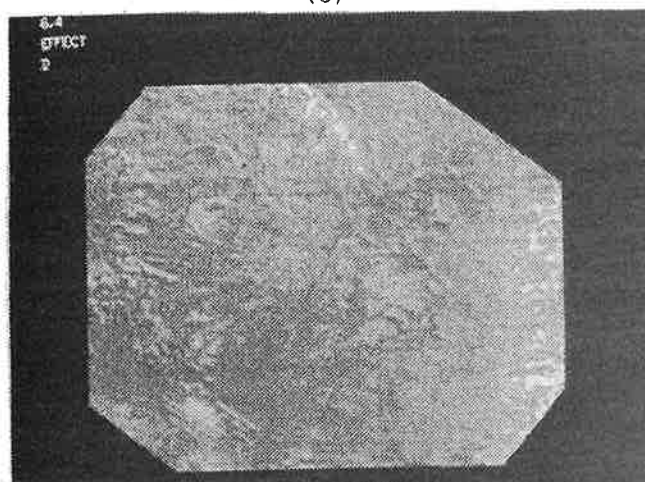


Figure 8: (a) SIR-B SAR image is  $20 \times 20$  sq km near San Jose de San Martin, Argentina; (b) geometrically rectified (geo-coded); (c) radiometrically rectified (See also Domik et al., 1986).



Table 2: SIR-B stereo-coordinate accuracies obtained from image pairs as listed by data takes.

Area	Stereo-model Data take	Inter-section angle (°)	Coordinate errors in meters		
			North	East	Height
Gordon la	04/88	5	67	78	86
Graza	88/72	8	78	70	110
	72/56	10	65	86	67
	104/72	13	77	73	65
	88/56	18	59	74	59
	104/56	23	62	49	62
Mt. Shasta	39/55	6	106	106	125
	55/87	23	44	75	53
	39/87	28	91	100	73
Illinois	49/97	57	240	185	10
Jose de San Martin	92/76	11	72	118	26
	56/72	11	76	155	42
Australia	17/36	15	93	80	36
	36/10	19	61	77	45
	17/10	32	58	107	22

## 5. CONCLUSIONS

Early non-radargrammetric SAR-mapping projects in 1970-1975 neglected any geometric rigor or adherence to cartographic standards. Currently, however, the advent of INS/GPS, of digital SAR and of satellite platforms in polar orbits combine to push SAR nearer to an operational use of radargrammetric concepts.

We have reviewed 3 specific applications areas that one might relate to mapping: creating a 1:50,000 image map, sea-ice motion mapping, and geometric as well as radiometric preparation of SAR images for subsequent analysis of image contents.

These applications would be insignificant, were it not for the pending arrival of several Earth and Venus-orbiting satellite radars. One must expect that a continuous stream of SAR data will be generated, irrespective of weather or day/night. Radargrammetric work will support the use of images in earth science disciplines, and it will stand on its own in sea-ice mapping and in creating SAR image maps at scale 1:50,000.

## ACKNOWLEDGEMENT

This paper uses results of work contributed by Dr. G. Domik, R. McConnell, E. Kienegger, W. Mayr, J. Coe and D. Allen, all of VEXCEL. Funding was from various sources, in particular from the Jet Propulsion Laboratory in Pasadena, CA, and from INTERA Technologies Ltd. of Calgary, Canada. The support is gratefully acknowledged.

## REFERENCES

- Domik, G., F. Leberl, and J. Cimino (1986) "Multiple Incidence Angle SIR-B Experiment over Argentina: Generation of Secondary Image Products," IEEE Trans. Geoscience Remote Sensing, Vol. 24, No. 4.
- Leberl, F., M.L. Bryan, Ch. Elachi, T. Farr, W. Campbell (1979) "Mapping of Sea-ice and Measurement of its Drifts Using Aircraft Synthetic Aperture Radar Images," J. Geophysical Research, 84 (C4): pp. 1827-1935.
- Leberl, F., J. Raggam, C. Elachi, and W.J. Campbell (1983) "Sea Ice Motion Measurements from SEASAT SAR Images," Journal of Geophysical Research, 88 (c3): 1915-1928.
- Leberl, F. (1982) "The Applicability of Satellite Remote Sensing to Small and Medium Scale Mapping." Proceedings. EARSel EASA Symposium on Satellite Remote Sensing or Developing Countries, Iqis. 20-21 April. ESA-SP-175, S. 81-85.
- Raggam, J., F. Leberl (1984) "SMART--A Program for Radar Stereo Mapping on the Kern DSR-1," Proceedings, Ann. Conv. of the Am. Soc. of Photogrammetry, pp. 765-773.
- Vesecki, J.F. et al. (in print) "Observation of Sea-ice Dynamics using Synthetic Aperture Radar Images: Automated Analysis." IEEE Trans. Geoscience and Remote Sensing.